International Journal of Innovative Computing, Information and Control
Volume **9**, Number **1**, January **2013**

ICIC International ©2013 ISSN 1349-4198
pp. 287–303

GRAVITY COMPENSATION FOR AN ILPMSM DRIVER BASED ON A ROBUST UNCERTAINTY CONTROLLER WITH SYSTEM DELAY COMPENSATION

Wei-Hann Yao[1], Pi-Cheng Tung[1,*], Chyun-Chau Fuh[2] and Fu-Chu Chou[1]

[1]Department of Mechanical Engineering
National Central University
No. 300, Jhongda Rd., Jhongli City, Taoyuan County 32054, Taiwan
*Corresponding author: t331166@ncu.edu.tw

[2]Department of Mechanical and Mechatronic Engineering
National Taiwan Ocean University
No. 2, Beining Rd., Keelung 20224, Taiwan
f0005@mail.ntou.edu.tw

Received October 2011; revised February 2012

Abstract. *Gravity compensation for an ironless linear permanent magnet synchronous motor (ILPMSM) driver based on a robust uncertainty controller with system delay compensation is presented. In the proposed control scheme, the robust uncertainty controller includes an inverse of the designed first order reference model with an input deduction and integral term; the system delay compensation adopts an inverse system delay model to compensate the system transport delay effect. The proposed controller can reduce disturbance and modeling uncertainty due to the difference between the reference model and the real system model, and the proposed controller does not require knowing precise system parameters. The system response that can be achieved is similar to that of the designed reference model, where DC gain is one. Therefore, DC gain of the controlled closed-loop system is denoted as one, so the proposed controller does not need to be combined with other control algorithms. In this paper, first, the proposed control scheme is used for ILPMSM system current control to reduce disturbance due to the d-q axis coupling effect and modeling uncertainty. Next, it is used for ILPMSM system velocity control to reduce modeling uncertainty and disturbances of friction and gravity force. The effectiveness of the proposed control scheme is verified by the simulation and experimental results.*
Keywords: Gravity compensation, Linear motor, Robust uncertainty controller, Delay compensation

1. **Introduction.** Linear electric motors can drive a linear motion load without intermediate gears or power screws. Therefore, linear motors are being increasingly used as actuators in many automation control fields, including manufacturing industries, machining tools, and transportation systems. Linear synchronous motors (LSMs) and linear switched reluctance motors (LSRMs) are used for vertical linear transportation applications such as ropeless elevators [1-4]. For linear motors to achieve perfect performance in terms of velocity and position control, excellent winding current control is the first and most important issue. However, the current control performance of the linear motor system can be affected by uncertainty of the current system parameters and back electromotive force (EMF). In the velocity loop, modeling uncertainty and disturbances of friction and gravity force can reduce the velocity control performance. For machine tool systems with high speed linear motors, gravity compensation of the z-axis is important to maintain the system performance.

From a survey of the existing researches on high performance motor control systems, it is found that a sliding-mode-observer-based adaptive control for a servo actuator control system was proposed in [5], where a sliding-mode observer was proposed to estimate the internal friction state of the LuGre model. Based on the estimated friction state, adaptation laws were designed to compensate for the unknown friction and load torque. In [6], an adaptive fuzzy controller constructed by a fuzzy basis function and a parameter-adjustable mechanism was derived and applied to the position loop of the PMLSM driver to cope with dynamic uncertainty and external load. In [7], a field-programmable gate array (FPGA)-based adaptive backstepping control system with a radial basis function network (RBFN) observer was proposed to control the mover position of a linear induction motor (LIM). Lin et al. at [8] investigated the scheme of a modified Elman neural network controller to control the mover of a permanent magnet linear synchronous motor (PMLSM) servo driver to track periodic reference trajectories. A recurrent functional link (FL)-based fuzzy neural network (FNN) controller was proposed in that study to control the mover of a permanent-magnet linear synchronous motor (PMLSM) servo driver to track periodic reference trajectories [9]. A sliding-mode control with a double boundary layer for robust compensation of payload mass and friction for a tubular linear synchronous motor (TLSM) aiming for highly accurate and robust position tracking with micrometric tolerances was proposed in [10]. In [11], a function-based sliding-mode control (SMC) method and direct thrust control (DTC) for position control in a real-world permanent-magnet linear synchronous motor (PMLSM) were proposed. In [12], an adaptive robust positioning control for an LPMSM drive based on an adaptive inverse model and robust disturbance observer was proposed. A digital positioning control for an LPMSM drive with quantitative and robust response under unknown mass and large command was proposed in [13]. A field-programmable gate array (FPGA) based robust radial basis function network (RBFN) control system was proposed to control the mover position of a linear induction motor [14]. In [15], a field-programmable gate array (FPGA)-based intelligent-complementary sliding-mode control (ICSMC) was proposed for control of the mover of a permanent magnet linear synchronous motor (PMLSM) servo-drive system to track periodic-reference trajectories. A hybrid fuzzy-PI speed controller with the three switching functions for PM synchronous motor speed control was proposed in [16].

To suppress the gravity effects, two inverse Jacobian regulators with gravity compensations were proposed for robot arm control in [20]. In [21], a simple extension of the PD-with-gravity-compensation control law was proposed. Also, an asymptotic stable proportional derivative control with sliding mode gravity compensation and with a high gain observer for robotic arms was proposed, recently. For machine tool systems with high speed linear motors, an active pneumatic control system for the weight compensation of the z-axis driven by a high speed linear motor was proposed in [22]. The active pneumatic control system was controlled by a self-tuning neural fuzzy control method.

In this paper, gravity compensation for an ILPMSM driver based on a robust uncertainty controller with system delay compensation is proposed. The proposed controller does not require knowing precise system parameters. This proposed controller will allow system steady-state output to be equal to input, which means that DC gain of the closed-loop controlled system is designed as one, so it does not need to be combined with other control algorithms. In this paper, the proposed control scheme is first applied for ILPMSM system current control to reduce disturbance due to the d-q axis coupling effect and modeling uncertainty. Next, it is applied for ILPMSM system velocity control to reduce modeling uncertainty and disturbances of friction and gravity force. The proposed control scheme of gravity compensation can be realized for the z-axis of machine tool systems with high speed linear motors and ropeless elevators.

2. **DSP-Based ILPMSM Driver.** Figure 1 shows the architecture of the proposed DSP-based ILPMSM driver, in which the d-q axis proposed controller, the velocity proposed controller, space-vector pulse width modulation (SVPWM) generator, Clarke transformation, park transformation and inverse park transformation are all implemented in a TMS320F2812 DSP chip. The TMS320F2812 DSP chip is manufactured by Texas Instruments Company.

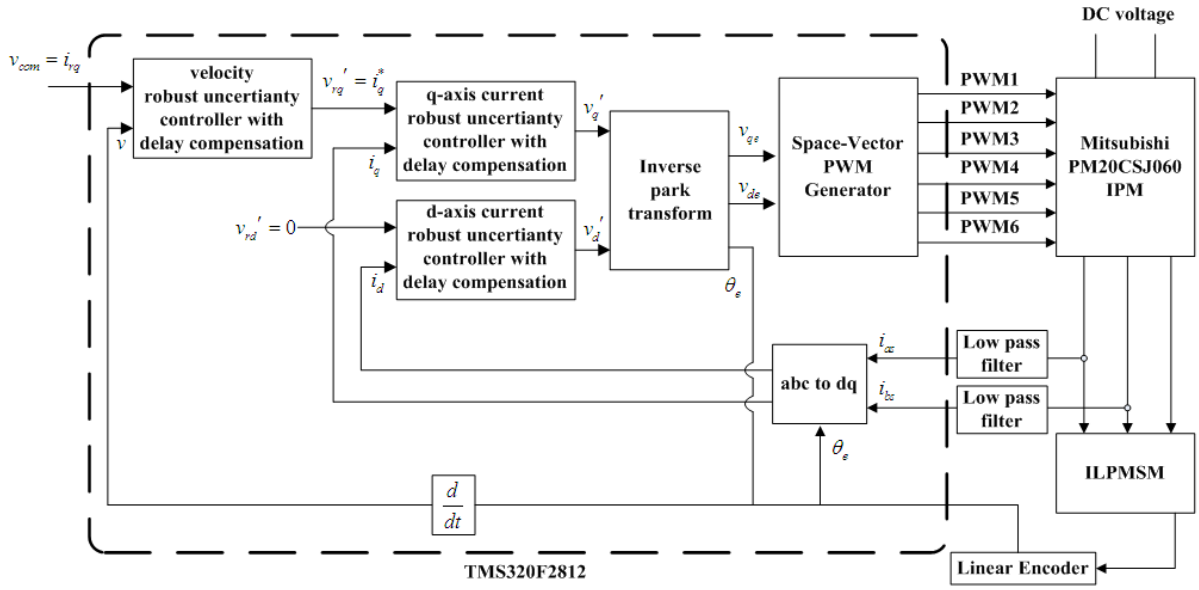

FIGURE 1. DSP-based ILPMSM driver

The inverter (PMS20CSJ060) in Figure 1 is manufactured by Mitsubishi, Japan. It is an intelligent power module (IPM) with input AC three-phase voltage max to 600 V, output current max to 20 Amps and max PWM input frequency to 20 kHz.

The ILPMSM in Figure 1, manufactured by Kollmorgen Company, USA, has no slots for the coil windings. The modular magnet array consists of two opposing rows of magnets to maximize the generated thrust force and to provide a flux return path for the magnet circuit. Kollmorgen ILPMSMs are rated as having a continuous force of 122 N and a peak force of 400 N.

3. **Dynamic Modeling.** The mathematical model of a typical ILPMSM is described in a d- and q-axis synchronous rotating reference frame. The voltage equations of three-phase symmetrical armature winding ILPMSM can be expressed as [17,18]:

$$\begin{aligned} V_d &= L_d \frac{d}{dt} i_d + R_d i_d + emf_d, \\ emf_d &= -\frac{\pi}{\tau} v L_q i_q \end{aligned} \tag{1}$$

$$\begin{aligned} V_q &= L_q \frac{d}{dt} i_q + R_q i_q + emf_q, \\ emf_q &= \frac{\pi}{\tau} v (L_d i_d + \lambda) \end{aligned} \tag{2}$$

where $V_d(V_q)$ denotes d-(q-) axis voltage, $L_d(L_q)$ denotes d-(q-) axis inductance, $i_d(i_q)$ denotes d-(q-) axis current, $R_d(R_q)$ denotes d-(q-) axis resistance, $emf_d(emf_q)$ is the d-(q-) axis back EMF, λ denotes flux linkages of the permanent magnet, τ denotes pole pitch, and v denotes ILPMSM velocity.

Figure 2 shows the d-axis current open loop of V_d to i_d and q-axis current open loop of V_q to i_q, where $v_d'(v_q')$ is the d-(q-) axis control force calculated by the robust uncertainty controller, k_{pwm} is the transfer factor of the PWM modulator, and $emf_d(emf_q)$ is the d-(q-) axis back EMF. After the transfer factor of the PWM modulator, the V_d' and V_q' voltages become the d- and q-axis voltages V_d and V_q, as shown in Equations (1) and (2) and in Figure 2. Thus the d-(q-) axis voltages of the armature windings are marked as V_d^* and V_q^* in Figure 2.

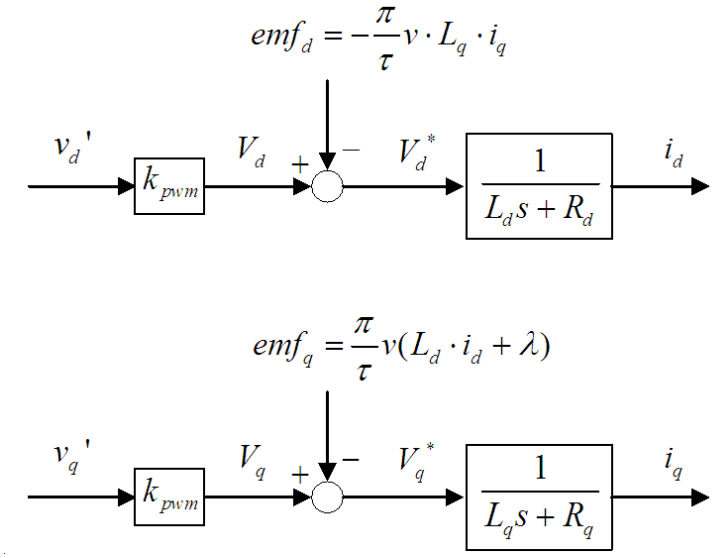

FIGURE 2. d-axis current open loop block diagram of V_d to i_d and q-axis current open loop block diagram of V_q to i_q

The electromagnetic developed force of an ILPMSM can be expressed as:

$$F_e = \frac{3}{2}\frac{\pi}{\tau}\left[\lambda i_q + (L_d - L_q) i_d i_q\right]. \tag{3}$$

The current control of an ILPMSM drive is based on zero direct axis current control in order to achieve the maximum electromagnetic developed force [17]. Therefore, the direct axis current i_d is equal to zero for direct axis current control. When $i_d \approx 0$, the force equation can be approximately written as:

$$F_e \triangleq \frac{3}{2}\frac{\pi}{\tau}\lambda i_q \triangleq K_t i_q, \tag{4}$$

where K_t is the force constant. Equation (4) shows that the electromagnetic developed force F_e is a direct ratio with the q-axis current.

The mechanical equation can be written as:

$$F_e - F_d = M\frac{dv}{dt} + Dv, \tag{5}$$

where M is the total mass of the moving part, D is the viscous friction coefficient, v is the ILPMSM mechanical velocity and F_d is the disturbance force, including gravity force and other friction force.

4. **Proposed Control Scheme.** Consider a plant $P(s)$, and a first order system that can be expressed as

$$P(s) = \frac{c}{s + b}, \tag{6}$$

where the parameters b, c are unknown positive constants and $b \neq c$.

Figure 3 shows the block diagram of the proposed control scheme for controlling $P(s)$, where k is a designed integral gain, which is a positive constant. $\hat{P}(s)$ is the designed first order reference model and can be expressed as

$$\hat{P}(s) = \frac{a}{s+a},$$

where a is a positive constant.

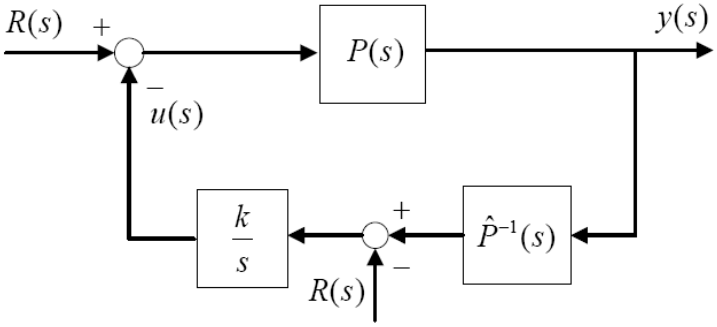

FIGURE 3. Proposed control scheme for controlling $P(s)$

It is noted that the order of the reference model must be the same as that of the system model for the proposed control scheme. As generally recognized, the low-pass filter is employed to realize the differentiator in the inverse reference model $\hat{P}^{-1}(s)$ [12]. The low-pass filter makes the transfer function of $\hat{P}^{-1}(s)$ proper and the causality is not violated.

The closed-loop transfer function of $R(s)$ to $Y(s)$ can be simplified as

$$G(s) = \frac{Y(s)}{R(s)} = \frac{acs + ack}{as(s+b) + kc(s+a)}. \tag{7}$$

When $k > 0$, the closed-loop transfer function of $R(s)$ to $Y(s)$ is a stable system.

The final value of $y(t)$ can be proved by the final value theorem when $R(s)$ is a unit step input,

$$\lim_{t\to\infty} y(t) = \lim_{s\to 0} \frac{1}{s} sG(s) = \frac{ack}{ack} = 1. \tag{8}$$

This result shows that the proposed control scheme allows DC gain of the controlled closed-loop system to be denoted as one. Equation (7) can be written as

$$G(s) = \frac{a}{s + a(\frac{bs+kc}{as+kc})}(\frac{cs+kc}{as+kc}). \tag{9}$$

Equation (9) shows that when k is designed to be larger, the response of $G(s)$ will be more closer to that of $\hat{P}(s)$ and can be rewritten as

$$G(s) \cong \frac{a}{s+a},$$

if k is very large. It implies that the system response is similar to that of the designed reference model.

The designed reference model $\hat{P}(s)$ is different from the real model $P(s)$; there exists an error between them. If we consider the designed reference model as the modeling system, and the modeling uncertainty ρ can be treated as the input to the modeling system, then

Figure 3 can be re-expressed as Figure 4, with unknown disturbance d considered. The modeling uncertainty ρ can be defined as follows, from Figure 4:

$$\begin{aligned} y &= P(s)U, \\ y &= \hat{P}(s)(U+\rho), \\ P(s)U &= \hat{P}_d(s)(U+\rho), \\ \rho &= \frac{[P(s)-\hat{P}(s)]}{\hat{P}(s)}U. \end{aligned}$$

The compensation force $u(s)$ of the proposed controller is given by

$$\begin{aligned} u &= \frac{k}{s}\left[U+\rho-R\right], \\ &= \frac{k}{s}\left[d+\rho-u\right], \\ &= \frac{k}{s+k}\left[d+\rho\right]. \end{aligned} \tag{10}$$

Hence, the compensation force u tracks the sum of the unknown disturbance and the unknown parameter uncertainty function due to modeling uncertainties if k is very large. To ensure that this control force can be effectively used to reduce the influence of the modeling uncertainties acting on the plant, the residual uncertainties v_u of the proposed controller can be written as

$$v_u = d+\rho-u = \frac{s}{s+k}\left[d+\rho\right], \tag{11}$$

showing that when the designed value of k is larger, the performance of uncertainties cancellation can be improved and the system response is similar to that of the designed model.

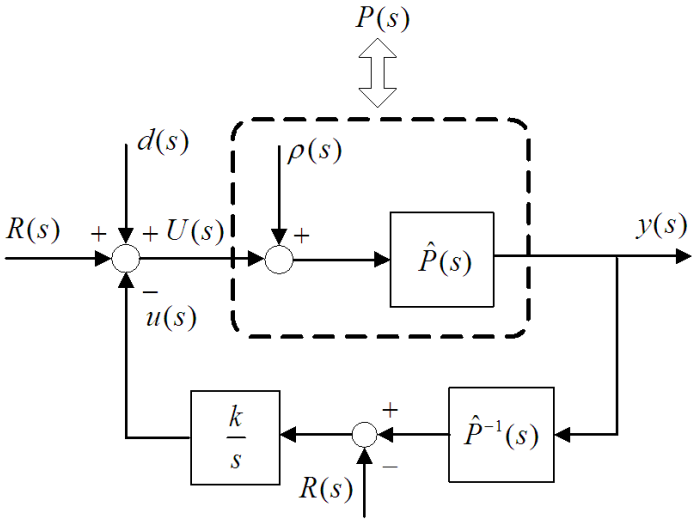

FIGURE 4. Proposed control scheme for controlling $P(s)$ with disturbance

4.1. **Robust uncertainty control scheme for current control [19].** The proposed control scheme is applied for ILPMSM system current control to reduce disturbance due to the d-q axis coupling effect and modeling uncertainty as shown in Figure 5. Figure

5 shows the block diagram of the proposed controller with delay compensation of d-axis and q-axis current control. $E_d(E_q)$ is related to back EMF and can be treated as unknown disturbance due to the coupling effect; $v'_{rd}(v'_{rq})$ is the d-(q-) axis reference voltage command; $v'_d(v'_q)$ is the d-(q-) axis control force of the proposed controller; $u_{Cd}(u_{Cq})$ is the d-(q-) axis compensation force of the proposed controller; and $\hat{P}_d(s)(\hat{P}_q(s))$ is the transfer function of the design reference model. $i_d(i_q)$ is the d-(q-) axis current. Because the d-(q-) axis current is transformed by ILPMSM armature winding measure current i_a and i_b, an analog low pass filter is added in i_a and i_b current measurement circuits as shown in Figure 1 in order to suppress the high frequency noises and is employed to realize the differentiator in the inverse reference model $P_d^{-1}(s)(P_q^{-1}(s))$. $P_d(s)(P_q(s))$ is the unknown d-(q-) axis current real model, which can be rewritten as

$$P_d(s) = \frac{k_{PWM}}{L_d s + R_d}, \quad P_q(s) = \frac{k_{PWM}}{L_q s + R_q}.$$

In Figure 5, e^{-Ls} is the system transport delay, and L is the system transport delay time, where $L = 0.00005$ second in the experiment of current loop. It should be noted that the system transport delay will degrade the system performance and cause system response overshoot. Therefore, the proposed approach adds a delay compensation term which consists of the inverse system transport delay model e^{Ls} in front of the robust uncertainty controller. The delay compensation term can be expanded by Taylor series as

$$e^{Ls} = 1 + \frac{Ls}{1!} + \frac{L^2 s^2}{2!} + \frac{L^3 s^3}{3!} + \cdots \approx 1 + Ls.$$

The high order terms are near to zero, since the value of the delay is very small, so they can be ignored. The system transport delay will be canceled by the delay compensation term in Figure 5 due to the fact that

$$e^{-Ls} \cdot e^{Ls} \approx 1.$$

This approximation is satisfactory only with very small delays.

Just as Figure 3 can be re-expressed as Figure 4, Figure 5 can be re-expressed as Figure 6. If the uncertainty ρ_d and ρ_q can be compensated by the robust uncertainty controller, then the system response can be similar to that of the designed model $\hat{P}_d(s)$ and $\hat{P}_q(s)$.

Since the disturbance, uncertainty and delay can be cancelled mostly by the proposed controller and delay compensation of the current loop, the d-(q-) axis model finally can be simplified to approximate an ideal first order system $\hat{P}_d$ and $\hat{P}_q$ as shown in Figure 7. This means DC gain of the controlled system is denoted as one. Therefore, v'_{rd} and v'_{rq} can represent d-axis current command i_d^* and q-axis current command i_q^*.

4.2. **Robust uncertainty control scheme for velocity control.** When the d-(q-) axis model finally can be simplified to an ideal first order system $\hat{P}_d$ and $\hat{P}_q$, the robust uncertainty control scheme is applied for ILPMSM system velocity control to reduce modeling uncertainty and disturbances of friction and gravity force. Figure 8 shows the block diagram of the proposed controller with delay compensation of velocity control, where F_d is related to friction and gravity force and can be treated as disturbance; K_t is the force constant as shown in Equation (4); i_{rq} is the reference current command and can represent velocity command v_{com}; i_q^* is the control force of the robust uncertainty velocity controller and can represent q-axis current command; and i_q is the q-axis measure current. Because the q-axis current response finally can be simplified to an ideal first order system $\hat{P}_q(s)$, it is faster than the mechanical system. The sampling frequency of the current loop is 20 kHz, but the sampling frequency of the velocity loop is 1 kHz. Thus in the velocity

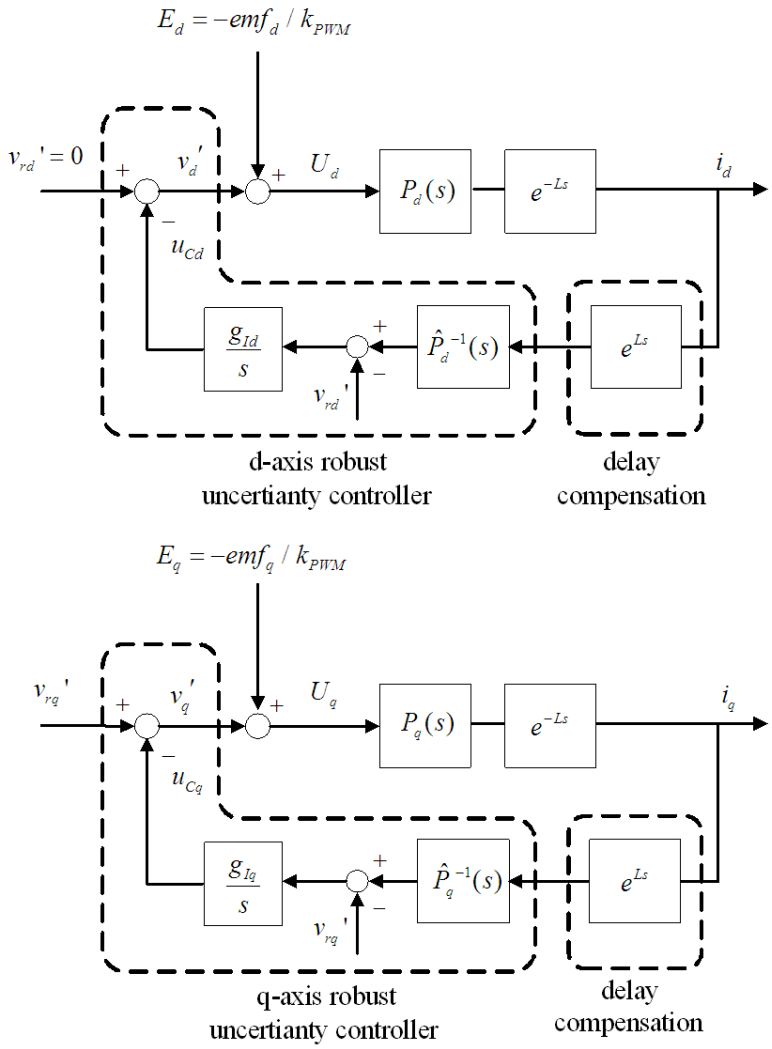

FIGURE 5. d-axis and q-axis robust uncertainty controller with system delay compensation

loop, the q-axis current response can be simplified to 1, which means $i_q \approx i_q^*$; u_C is the compensation force of the proposed controller; v is the measured velocity; $\hat{P}_m(s)$ is the designed first order reference model of the velocity loop; and $P_m(s)$ is the real mechanical dynamic model of Equations (4) and (5), which can be expressed as

$$P_m(s) = \frac{1}{Ms + D},$$

where K_t is the force constant as shown in Equation (4), and the system parameters of M, D and K_t are all unknown. It should be noted that F_d is moved to the left side of block K_t and re-expressed as $\frac{F_d}{K_t}$.

In Figure 8, $e^{-L's}$ is the system transport delay, and L' is the system transport delay time, where $L' = 0.001$ second in the velocity loop experiment. The system transport delay will be canceled by the delay compensation term in Figure 8 due to the fact that

$$e^{-L's} \cdot e^{L's} \approx 1.$$

The low-pass filter in Figure 8 is employed to realize the differentiator in the inverse reference model $\hat{P}_m^{-1}(s)$.

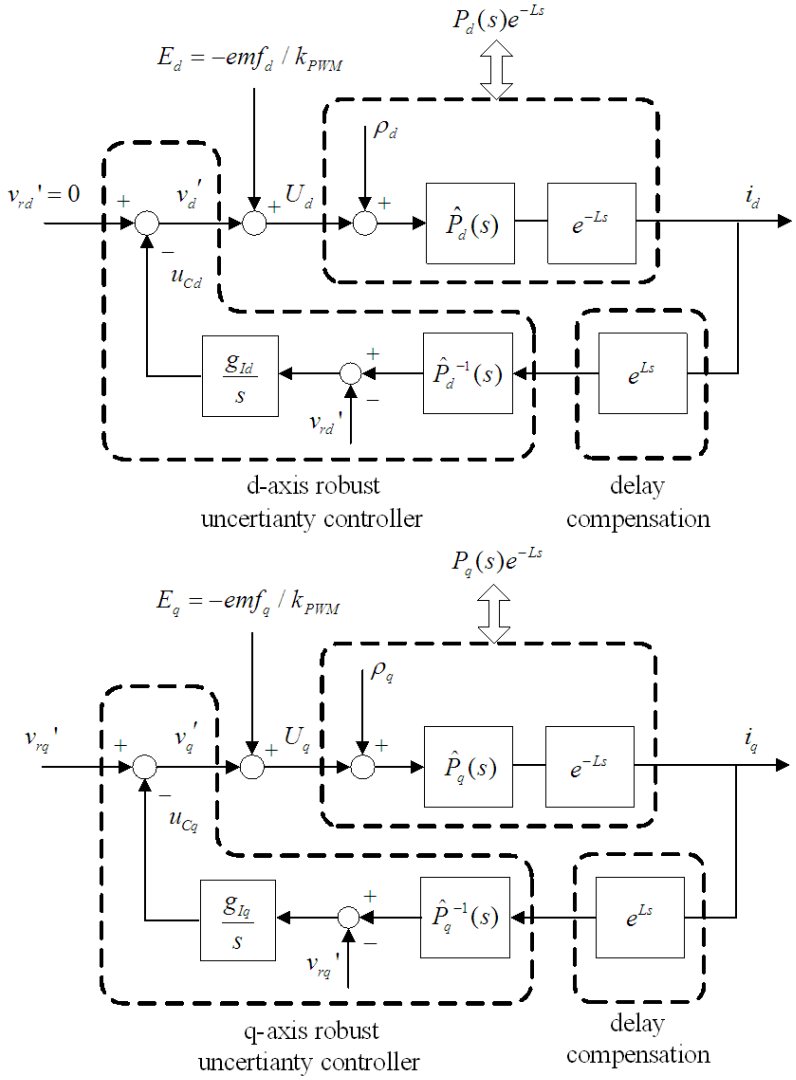

FIGURE 6. d-axis and q-axis robust uncertainty controller with system delay compensation

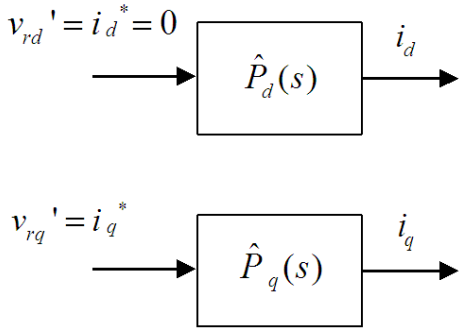

FIGURE 7. Simplified d-axis and q-axis current model from Figure 6

Figure 8 can be re-expressed as Figure 9. If the uncertainty ρ_v can be compensated by the robust uncertainty controller, then the system response can be similar to that of the designed model $\hat{P}_m(s)$.

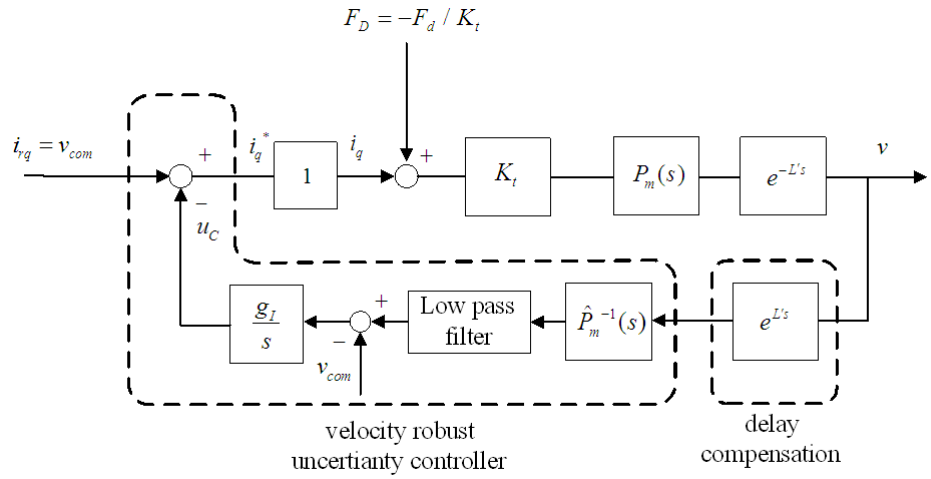

FIGURE 8. Velocity robust uncertainty controller with system delay compensation

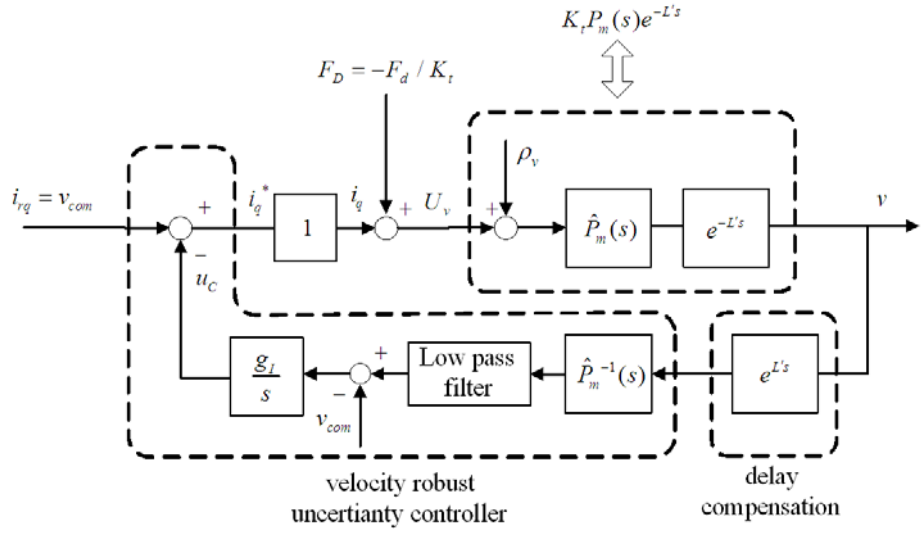

FIGURE 9. Velocity robust uncertainty controller with system delay compensation

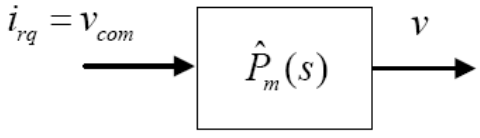

FIGURE 10. Simplified velocity model from Figure 9

Since the disturbances, uncertainties, and delay can be cancelled mostly by the proposed controller and delay compensation of the velocity loop, the velocity model includes the current model and finally can be simplified to approximate an ideal first order system $\hat{P}_m(s)$ as shown in Figure 10.

5. **Simulation Results.** The simulation results show the comparison of the proposed controller without disturbance and gravity force and the proposed controller with disturbance and gravity force in velocity control.

Consider a linear motor mechanical dynamic model $K_tP(s)$, which can be expressed as

$$K_tP(s) = \frac{15}{s+10},$$

the reference model of the proposed controller is

$$\hat{P}(s) = \frac{50}{s+50},$$

integration gain of the proposed controller is

$$k = 50000$$

and disturbance is $d = 50\sin(100t)$ (N).

Consider the linear motor system to be perpendicular to the ground; the gravity force is 100 (N).

In Figure 11, the dashed line denotes the command, which is 0.05 (m/s). The solid line denotes the response by using the proposed controller without disturbance and gravity force; the response is close to that of the reference model. The dotted line denotes the response by using the proposed controller with disturbance and gravity force; the response is still close to that of the reference model. The results of this simulation show the good disturbance reduction effect of the proposed controller.

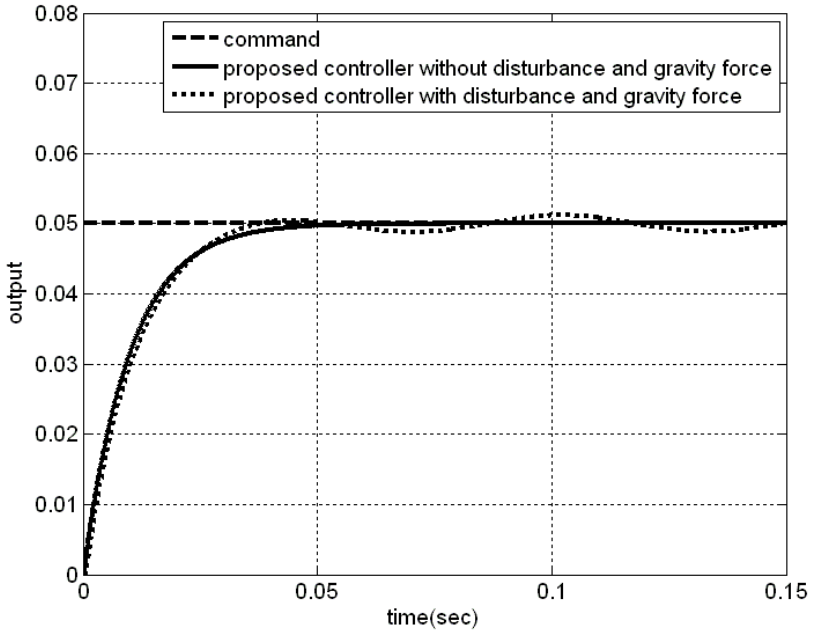

FIGURE 11. Simulation results

6. **Experimental Results.** Figures 12, 13 and 14 present photographs of our experimental setup. Figure 12 shows the DSP-based motor driver, Figure 13 shows the ILPMSM system horizontal to the ground and Figure 14 shows the ILPMSM system vertical to the ground. In the experiment, the sampling frequency of the current loop is 20 kHz and the sampling frequency of the velocity loop is 1 kHz. The saturation values for control force of the robust uncertainty controller v_d' and v_q' are ± 2.5 volts. In the current loop, an analog low pass filter is added in i_a and i_b current measurement circuits as shown in Figure 1 in order to suppress the high frequency noises. The cutoff frequency of the analog low

pass filter is 234081 Hz, so the filter may not deteriorate the dynamic properties of the system. In the velocity loop, a digital low pass filter is added in order to reduce the high frequency noises of the inverse reference model output signal. The cutoff frequency of the digital low pass filter is 200 Hz, which is faster than the mechanical system. Therefore, the digital filter may not deteriorate the mechanical dynamic properties of the system. These low-pass filters make the inverse reference models of current loop and velocity loop proper.

The time responses of using the proposed controller of d-axis and q-axis current control and velocity control are plotted in Figure 15. The proposed controller of the current loop reference model $\hat{P}_d$, $\hat{P}_q$ is designed as

$$\hat{P}_d(s) = \frac{4000}{s+4000}, \quad \hat{P}_q(s) = \frac{4000}{s+4000},$$

and integral term gain is designed as $g_{Id} = 5000$ ($g_{Iq} = 5000$). The proposed controller of the velocity loop reference model is designed as

$$\hat{P}_m(s) = \frac{100}{s+100},$$

and integral term gain is designed as $g_I = 200000$. In order to design a suitable reference model for the proposed controller, it is necessary only to identify the system model roughly to obtain the time constant without knowing the system parameters precisely. It is noted that if the time constant of the designed reference model is too small or the integral term gain is too large, the effect will be bad, due to the fact that the control force will be in saturation. The specifications of the LPMSM system are listed in Table 1.

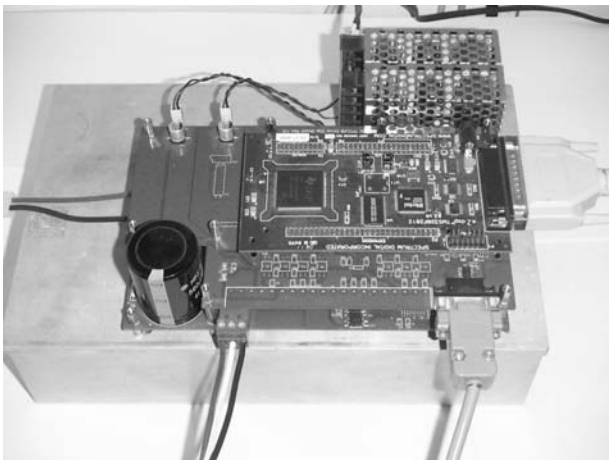

FIGURE 12. DSP-based motor driver

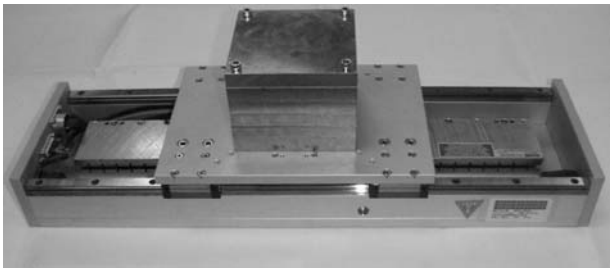

FIGURE 13. ILPMSM system horizontal to the ground

FIGURE 14. ILPMSM system vertical to the ground

TABLE 1. Parameters of the ILPMSM system

Symbol and name	Value	Unit
R_c electrical resistance	17.2	Ohms L-L
L electrical inductance	6.00	mH L-L
I_c continuous current	2.1	Arms
F_c continuous force	122	N
K_e Back EMF constant	57.0	Vpeak/m/s L-L
T_e electrical time constant	0.35	ms

In the experiment of Figure 15, the ILPMSM system is horizontal to the ground and the load is 3.4 kg. In Figure 15, the d-axis reference voltage command v'_{rd} is zero in order to keep d-axis current i_d near zero for zero direct axis current control. In Figure 15(a1), the d-axis current responses remain at zero. Figure 15(b1) shows the q-axis current i_q, and the q-axis reference voltage command $v'_{rq} = i^*_q$, where i^*_q is the control force of the velocity robust uncertainty controller in Figure 15(c3). Figure 16 shows the comparison of Figure 15(c3) and Figure 15(b1); the dashed line is the control force of the velocity robust uncertainty controller i^*_q, and it can be treated as the q-axis current command. The solid line in Figure 16 denotes the q-axis current response. This comparison result shows that the response of the q-axis current model can be simplified as one, which means the q-axis current is equal to the q-axis current command. Figure 15(c1) shows the ILPMSM system velocity v of a step command. The dashed line denotes a step command of velocity 0.05 m/s and the time constant of velocity step response is about 0.01 sec. This is quite close to the time constant of the reference model $\hat{P}_m$ in (1/100sec), and the steady-state velocity v is equal to the velocity command v_{com}. This experimental result shows superior performance of the proposed controller in the current loop and velocity loop.

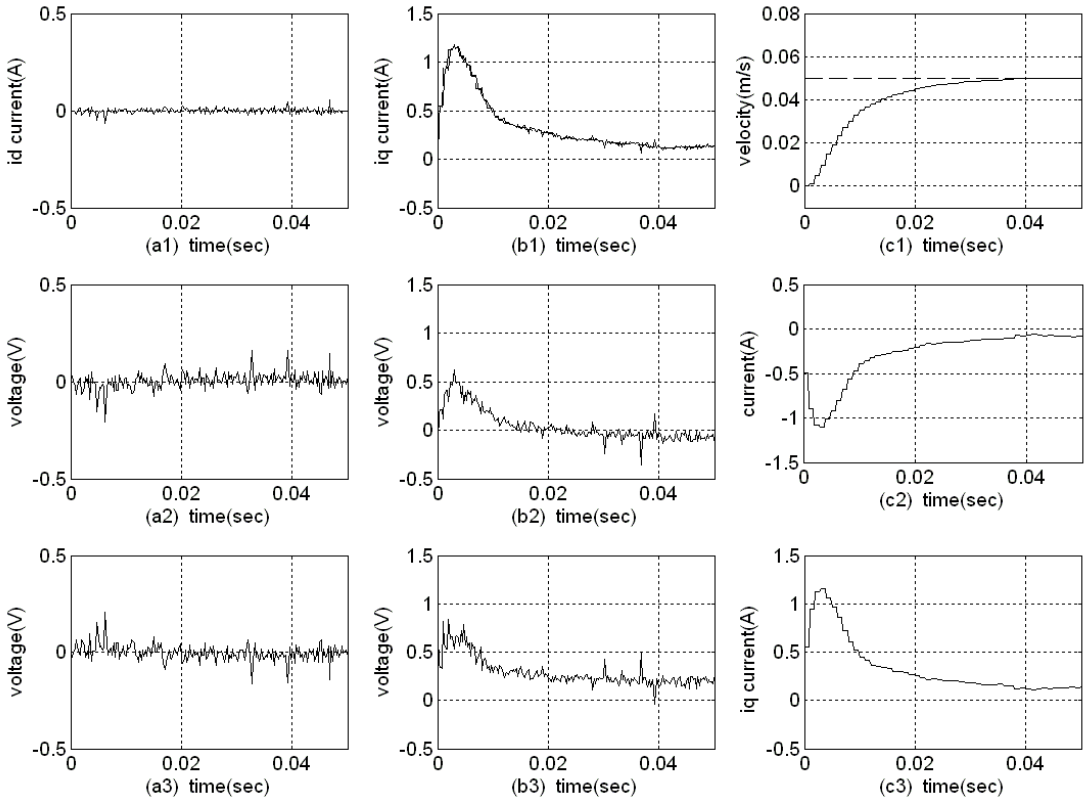

FIGURE 15. (a1) d-axis current i_d; (a2) d-axis compensation force of the robust uncertainty controller u_{Cd}; (a3) d-axis control force of the robust uncertainty controller v_d'; (b1) q-axis current i_q; (b2) q-axis compensation force of the robust uncertainty controller u_{Cq}; (b3) q-axis control force of the robust uncertainty controller v_q'; (c1) ILPMSM system velocity v of a step command; (c2) compensation force of the velocity robust uncertainty controller u_C; (c3) control force of the velocity robust uncertainty controller i_q^*

Figure 17(a) shows the velocity step response of the ILPMSM system horizontal to the ground of the proposed controller with different velocity reference models. The load of ILPMSM system is 3.4 kg and the other experimental parameters are the same as those in Figure 15. The velocity loop reference models are designed as

$$\text{designed reference model 1 } \hat{P}(s) = \frac{50}{s+50},$$
$$\text{designed reference model 2 } \hat{P}(s) = \frac{100}{s+100}.$$

In Figure 17(a), the solid line denotes the velocity step response of the designed velocity reference model 2, and the time constant of velocity step response is about 0.01 sec. This is quite close to the time constant of the designed reference model 2 in (1/100sec). The dotted line denotes the velocity step response of velocity reference model 1; the time constant of velocity step response is still quite close to the time constant of the designed reference model 1 in (1/50sec). These results show the system model response will follow that of the designed reference model perfectly.

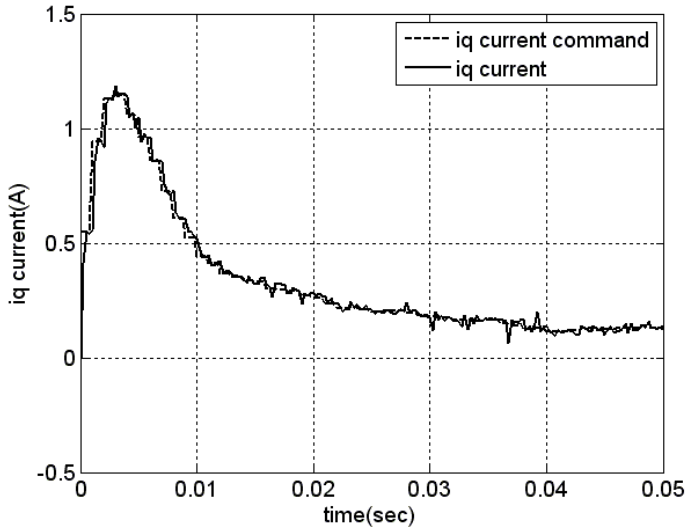

FIGURE 16. q-axis current response of the proposed controller

Figure 17(b) shows the velocity step response of the ILPMSM system vertical to the ground of the proposed controller with different velocity reference models. In this experiment, the mechanical load is zero, and the total mass of the moving part of the ILPMSM system is about 3.6 kg. The other experimental parameters are the same as in Figure 17(a). In Figure 17(b), the system model response still follows the designed reference model when the ILPMSM system is vertical to the ground. This result shows the excellent gravity compensation effect of the ILPMSM system velocity loop.

7. **Conclusions.** Gravity compensation for an ironless linear permanent magnet synchronous motor (ILPMSM) driver based on a robust uncertainty controller with system delay compensation has been presented. The proposed control scheme of gravity compensation can be used for the z-axis of machine tool systems with high speed linear motors and ropeless elevators. The experimental results show that the ILPMSM system current response and velocity response are similar to those of a designed ideal first order system whose DC gain is one by the proposed controller. Therefore, system steady-state output is equal to input for constant speed control, which means that DC gain of the controlled closed-loop system is designed as one. The experimental results also show that the proposed controller successfully reduces the disturbance due to the d-q axis coupling effect and modeling uncertainty of the current loop, and reduces modeling uncertainty and disturbances of friction and gravity force of the velocity loop.

Hence, the first advantage of the proposed controller is its relative simplicity, for it allows system steady-state output to be equal to input, which means that DC gain of the controlled system is designed as one. As a result, the proposed controller does not need to be combined with other control algorithms. The second advantage of the proposed controller is that it does not need to know system parameters precisely. Finally, the ILPMSM system velocity response can be similar to that of the designed velocity reference model. The good performance of the proposed controller is verified, and it is suitable for application to ILPMSM system velocity control.

Acknowledgments. This work was funded by National Science Council of Taiwan, under grant NSC-99-2221-E-008-029.

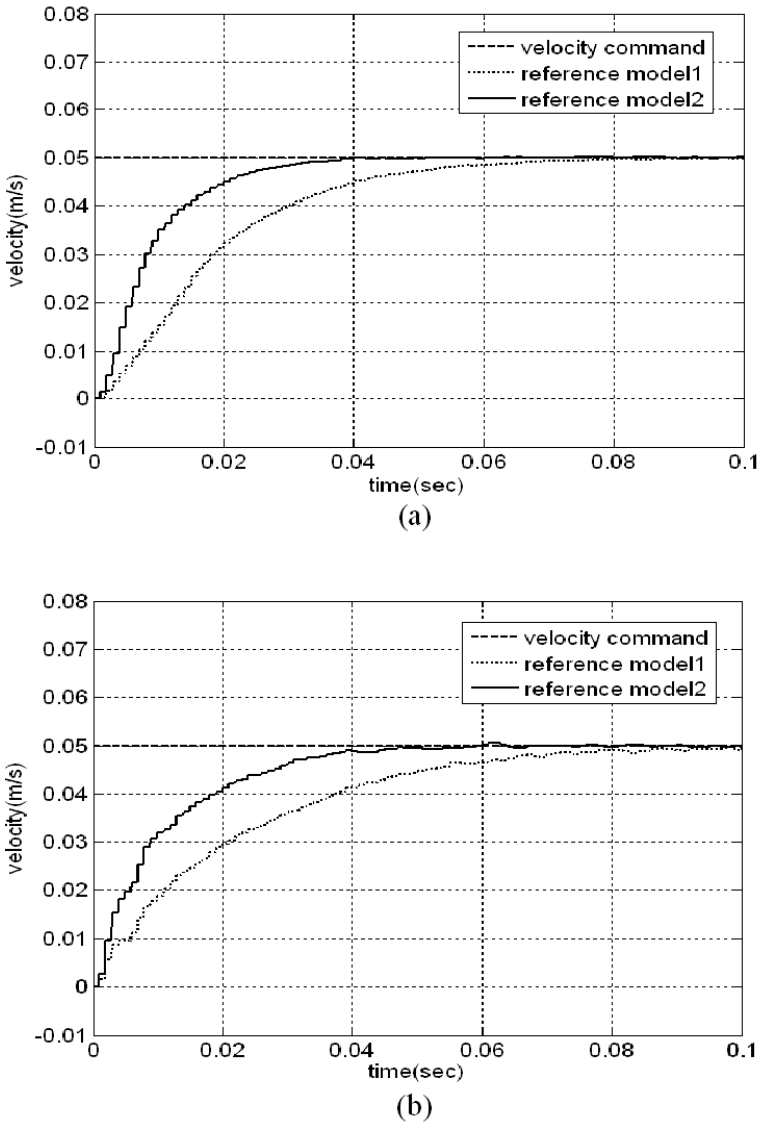

FIGURE 17. (a) Step response of ILPMSM system horizontal to the ground of the proposed controller and (b) step response of ILPMSM system vertical to the ground of the proposed controller

REFERENCES

[1] K. Yoshida and H. Matsumoto, Propulsion and guidance simulation of a high-temperature superconducting bulk ropeless linear elevator, *IEEE Transactions on Magnetics*, vol.40, no.2, pp.615-618, 2004.

[2] S. H. Lim and R. Krishnan, Ropeless elevator with linear switched reluctance motor drive actuation systems, *IEEE Transactions on Industrial Electronics*, vol.54, no.4, pp.2209-2217, 2007.

[3] N. S. Lobo, S. H. Lim and R. Krishnan, Comparison of linear switched reluctance machines for vertical propulsion application: Analysis, design, and experimental correlation, *IEEE Transactions on Industrial Applications*, vol.44, no.4, pp.1134-1142, 2008.

[4] S. H. Lim, R. Krishnan and N. S. Lobo, Design and control of a linear propulsion system for an elevator using linear switched reluctance motor drives, *IEEE Transactions on Industrial Electronics*, vol.55, no.2, pp.534-542, 2008.

[5] W. F. Xie, Sliding-mode-observer-based adaptive control for servo actuator with friction, *IEEE Transactions on Industrial Electronics*, vol.54, no.3, pp.1517-1527, 2007.

[6] Y. S. Kung, Design and implementation of a high-performance PMLSM drives using DSP chip, *IEEE Transactions on Industrial Electronics*, vol.55, no.3, pp.1341-1351, 2008.

[7] F. J. Lin, L. T. Teng, C. Y. Chen and Y. C. Hung, FPGA-based adaptive backstepping control system using RBFN for linear induction motor drive, *IET Electric Power Applications*, vol.2, no.6, pp.325-340, 2008.

[8] F. J. Lin, L. T. Teng and Y. C. Hung, Modified Elman neural network controller with improved particle swarm optimization for linear synchronous motor drive, *IET Electric Power Applications*, vol.2, no.3, pp.201-214, 2008.

[9] F. J. Lin, C. Y. Chen, L. T. Teng and H. Chu, Recurrent functional-link-based fuzzy neural network controller with improved particle swarm optimization for a linear synchronous motor drive, *IEEE Transactions on Magnetics*, vol.45, no.8, pp.3151-3165, 2009.

[10] F. Cupertino, D. Naso, E. Mininno and B. Turchiano, Sliding-mode control with double boundary layer for robust compensation of payload mass and friction in linear motors, *IEEE Transactions on Industrial Applications*, vol.45, no.5, pp.1688-1696, 2009.

[11] Y. S. Huang and C. C. Sung, Function-based controller for linear motor control systems, *IEEE Transactions on Industrial Electronics*, vol.57, no.3, pp.1096-1105, 2010.

[12] W. T. Su and C. M. Liew, Adaptive positioning control for a LPMSM drive based on adapted inverse model and robust disturbance observer, *IEEE Transactions on Power Electronics*, vol.21, no.2, pp.505-517, 2006.

[13] W. T. Su and C. M. Liaw, Robust balanced control of LPMSM servo drive with mass identification and large command change, *IEE Proc. of Electric Power Applications*, vol.153, no.3, pp.439-450, 2006.

[14] F. J. Lin, L. T. Teng, C. Y. Chen and C. K. Chang, Robust RBFN control for linearinduction motor drive using FPGA, *IEEE Transactions on Power Electronics*, vol.23, no.4, pp.2170-2180, 2008.

[15] F. J. Lin, J. C. Hwang, P. H. Chou and Y. C. Hung, FPGA-based intelligent-complementary sliding-mode control for PMLSM servo-drive system, *IEEE Transactions on Power Electronics*, vol.25, no.10, pp.2573-2587, 2010.

[16] A. V. Sant and K. R. Rajagopal, PM synchronous motor speed control using hybrid fuzzy-PI with novel switching functions, *IEEE Transactions on Magnetics*, vol.45, no.10, pp.4672-4675, 2009.

[17] P. C. Krause, O. Wasynczuk and S. D. Sudhoff, *Analysis of Electronic Machine and Drive Systems*, 2nd Edition, IEEE Press, New York, 2002.

[18] D. W. Novotny and T. A. Lipo, *Vector Control and Dynamics of AC Drivers*, Oxford University Press, Oxford, Britain, 1996.

[19] W. H. Yao, P. C. Tung, C. C. Fuh and F. C. Chou, A robust uncertainty controller with system delay compensation for an ILPMSM system with unknown system parameters, *IEEE Transactions on Industrial Electronics*, vol.58, no.10, pp.4727-4735, 2011.

[20] C. C. Cheah and H. C. Liaw, Inverse Jacobian regulator with gravity compensation: Stability and experiment, *IEEE Transactions on Robotics*, vol.21, no.4, pp.741-747, 2005.

[21] A. Zavala-Río and V. Santibáñez, Simple extensions of the PD-with-gravity-compensation control law for robot manipulators with bounded inputs, *IEEE Transactions on Control System Technology*, vol.14, no.5, pp.958-965, 2006.

[22] M. H. Tsai and M. C. Shih, A study of the pneumatic counterweight of machine tools conventional and active pressure control method, *JSME International Journal*, vol.49, no.3, pp.890-896, 2006.